The H.E.S.S. Project

Werner Hofmann, for the H.E.S.S. collaboration
Max-Planck-Institut für Kernphysik, D 69029 Heidelberg, P.O. Box 103989

1. Introduction

H.E.S.S. - the High Energy Stereoscopic System - is a system of four large imaging Cherenkov telescopes under construction in the Khomas Highland of Namibia, at an altitude of 1800 m. With their stereoscopic reconstruction of air showers, the H.E.S.S. telescopes provide very good angular resolution and background rejection, resulting in a sensitivity in the 10 mCrab range, and an energy threshold around 100 GeV. The H.E.S.S. experiment aims to provide precise spectral and spatial mapping in particular of extended sources of VHE gamma rays, such as Supernova remnants.

Construction of H.E.S.S. is well underway; the steel structures of all four telescopes have been erected and equipped with drive systems, the mirrors for all telescopes are in hand. The first H.E.S.S. telescope (Fig. 1) is fully operational and an inauguration ceremony took place at the H.E.S.S. site on Sept. 3, 2002. The site infrastructure is complete and includes a building with the experiment control room, offices, and workshops, a residence building, Diesel power generators and a Microwave tower linking the site to Windhoek and from there to the internet.

2. Telescope structures and drives

The H.E.S.S. telescopes use an alt-az mount, which rotates on a 15 m diameter rail. The steel structures are designed for high mechanical rigidity. Both azimuth and elevation are driven by friction drives acting on auxiliary drive rails, providing a positioning speed of 100°/min. Encoders on both axes give 10" digital resolution; with the additional analog encoder outputs, the resolution is improved by another factor 2 to 3. After initial tests and a few months of operation of the first telescope, the drives were slightly modified for smoother operation; the telescope design is now quite mature.

pp. 1–7

Fig. 1. The first complete H.E.S.S. telescope during the inauguration ceremony

3. Mirror

The mirror of a H.E.S.S. telescope is composed of 380 round facets of 60 cm diameter; the facets are made of ground glass, aluminized and quartz coated, with reflectivities in the 80% to 90% range. The facets are arranged in a Davies-Cotton fashion, forming a dish with 107 m^2 mirror area, 15 m focal length and $f/d \approx 1.2$.

To allow remote alignment of the mirrors, each mirror is equipped with two alignment motors with internal resolvers. The alignment procedure uses the image of a star on the closed lid of the PMT camera, viewed by a CCD camera at the center of the dish. The procedure is described in detail elsewhere in these proceedings. Fig. 2(left) shows the resulting intensity distribution, after all mirrors are aligned. The spot is well contained within a single hexagonal PMT pixel. As with all single-mirror designs, the spot width varies significantly with increasing distance from the optical axis. Fig. 2(right) shows the measured (points) and predicted (lines) spot width, both in terms of the radius containing 80% of the light, and in terms of the rms widths of the projected distributions. The measurements are in excellent agreement with simulations, indicating that the optical system and the alignment are well understood. Out to 2° from the optical axis, and hence over almost the entire field of view, the spot is essentially contained in a single pixel. Due to the superior quality of both the mirrors and the alignment system, the on-axis point spread function is significantly better than initially specified. The imaging qualities are stable over the elevation range from 30° to the zenith.

Telescope pointing was also verified using the images of stars on the camera lid. Without any corrections, star images were centered on the camera lid with a rms error of 28". Using a 12-parameter model to correct for misalignments of the

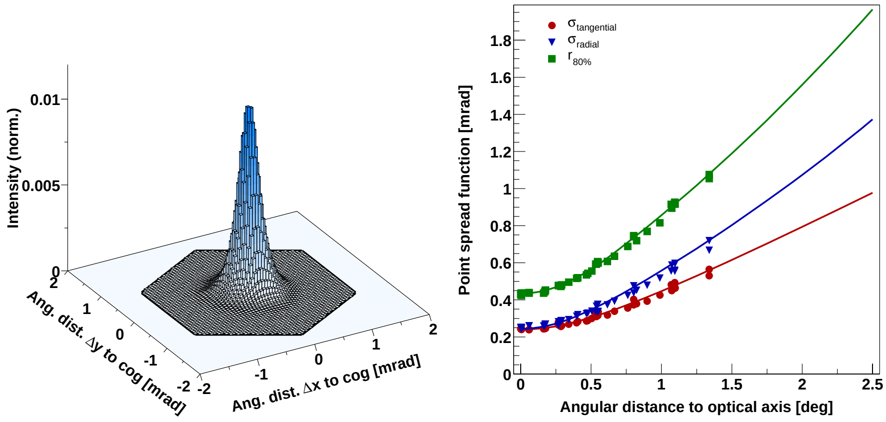

Fig. 2. Left: Image of a star on the camera lid, compared to the camera pixel size. Right: Mirror point spread function as a function of the angle to the optical axis. Shown are the 80% radius and the rms spot width after projection onto two orthogonal axes. Point represent measurements, lines the simulation.

telescopes axes etc., a pointing precision of 8" rms was reached. Finally, using a guide telescope attached to the dish for further corrections, the pointing was good to 2.5" rms. H.E.S.S. should therefore be able to locate gamma ray sources to a few arc-seconds.

4. Camera

The PMT cameras of the H.E.S.S. telescopes (Fig. 3) provide 0.16° pixel size over a 5° field of view, requiring 960 PMT pixels per telescope. The complete electronics for signal processing, triggering, and digitization is contained in the camera body; only a power cable and a few optical fibers connect the camera. For ease of maintenance, the camera features a very modular construction. Groups of 16 PMTs together with the associated electronics form so-called drawer modules, 60 of which are inserted from the front into the camera body, and have backside connectors for power, a readout bus, and trigger lines. The rear section of the camera contains crates with a PCI bus for readout, a custom crate for the final stages of the trigger, and the power supplies. The camera uses Photonis XP2960 PMTs, operated at a gain of $2 \cdot 10^5$. The PMTs are individually equipped with DC-DC converters to supply a regulated high voltage; for best linearity, the four last dynodes are actively stabilized.

The key element in the signal recording of the H.E.S.S. cameras is the ARS (Analog Ring Sampler) ASIC, which samples the PMT signals at 1 GHz and provides analog storage for 128 samples, essentially serving to delay the signal

Fig. 3. The camera of the first H.E.S.S. telescope.

until a trigger decision is reached. To provide a large dynamic range in excess of 10^4, two parallel high/low gain channels are used for each PMT. After a trigger decision, the pulse sampling is stopped, and the relevant storage locations are switched to an ADC for digitization. Under the control of an FPGA, the digitized pulse train can either be directly read out via a custom parallel bus (4 bus lines serve 15 drawers each), or the samples within a pre-defined integration window (currently 16 ns) can be added up and only the digital sum is read out. The full pulse shape readout is used primarily for diagnostic purposes; to reduce the data flow during normal operation, only the sum, i.e., the pulse area, is read out. Gains are adjusted such that a single photoelectron provides a signal of about 80 ADC channels. The high-gain channel has a linear range of 200 photoelectrons, with a noise of about 0.2 photoelectrons; the low-gain channel extends the linear range to 2000 photoelectrons. The drawer modules provide additional diagnostics such as PMT currents, PMT trigger rates, HV status and voltage, temperatures and more.

Currently, the camera is operated with trigger rates in the 100-150 Hz range and 20% deadtime, limited by the performance of the readout bus. Improved shielding of bus lines combined with a doubling of the number of buses should quadruple the speed in the near future.

A camera trigger is formed by a coincidence of some number of pixels (typically 3-5) within an 8x8 pixel group exceeding an adjustable threshold; typical operating thresholds are in the range of 3 to 5 photoelectrons. The pixel comparators generate a pixel trigger signal; the length of the signal reflects the time the input signal exceeds the threshold. Since typical noise signals barely exceed the threshold and result in short pixel trigger signals, the effective resolving time of the pixel coincidence is in the 1.5 to 2 ns range, providing a high suppres-

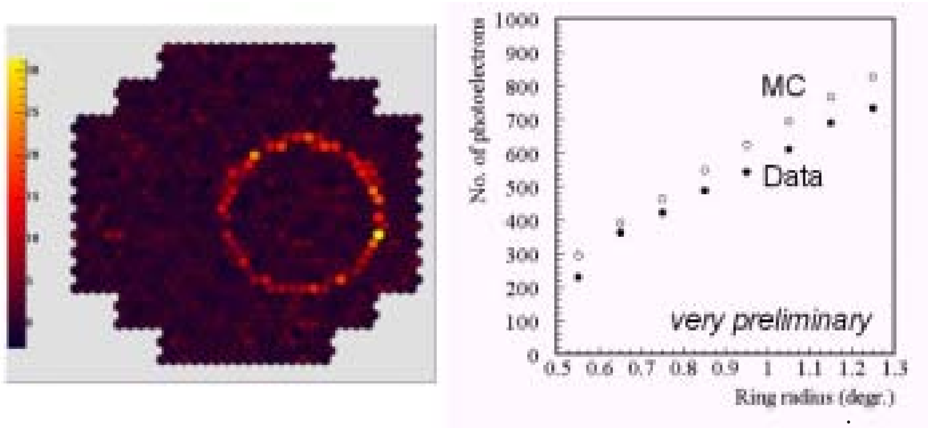

Fig. 4. (Left) A typical muon ring. (Right) Intensity of muon ring images, as a function of the ring radius. Full points: data, open points: simulation.

sion of random coincidences. Once more than one telescope is active, a central trigger coincidence will allow to impose arbitrary telescope configurations in the trigger, and to operate the telescopes either as a single four-telescope system, or as subsystems, up to four individual telescopes pointed at different objects.

5. First data

After the first telescope was equipped with mirrors in the fall of 2001, the camera was installed in May 2002 and first data were taken in June 2002. As expected for a single telescope, a significant fraction - roughly half - of the images are caused by muons, either in the from of full rings (Fig. 4(left)) or of short ring segments. The night-sky background - predicted to about 100 MHz photoelectron rate per pixel - induces a noise of 1.2 photoelectrons rms in the PMT pixels, consistent with expectations.

Muon rings were used to verify the overall performance and calibration of the telescopes. Rings were classified according to their radius - related to the muon energy - and by the impact parameter, which governs the intensity distribution along the ring. Fig. 4(right) shows, for well-contained rings, the total intensity in photoelectron units, as a function of ring radius, both for measured and simulated rings. The observed photoelectron yield agrees to better than 20% with expectations; at this stage of the commissioning, this should be considered a remarkably good agreement, and demonstrates that the optical system, the PMTs and electronics calibration are well understood.

Another important check for the performance of the telescope is the trigger rate, illustrated in Fig. 5 as a function of pixel trigger threshold. The rate varies

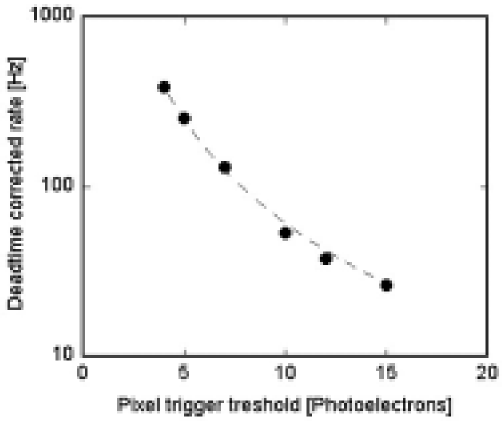

Fig. 5. Dead-time corrected trigger rate as a function of pixel threshold, for a four-pixel coincidence.

smoothly with threshold. Even for thresholds as low as four photoelectrons, trigger rates seem to be governed by air showers rather than by night-sky noise, which would induce a much faster variation with threshold. With a typical threshold of 4-5 photoelectrons, event size distributions peak around 100 to 150 photoelectrons; one photoelectron corresponds approximately to one GeV deposited energy.

Until mid-September 2002, about 65 h of on-source and off-source data were collected, observing objects such as SN 1006, RXJ 1713-3946, PSR B1706-44, the Crab Nebula, and NGC 253, PKS 2005-489, PKS 2155-304 as extragalactic source candidates. A significant fraction of the dark time was used for technical studies and calibration runs, or lost due to hardware and software commissioning and debugging. In particular the early physics data are of limited quality. Tools for data quality evaluation and data analysis are in the final stages of development; so far, only small subsets of the data have been processed. No statements concerning VHE gamma ray emission from the objects can be made at this time.

6. Conclusion

The first H.E.S.S. telescope is operational since June 2002, and first results concerning the technical performance of the telescopes, both concerning the optical system and the camera, look encouraging and did not expose major problems. Current schedules call for completion of the Phase-I four-telescope system in 2004. An expansion of the system - Phase II - with increased sensitivity is foreseen; the Phase II telescopes and their arrangement are under study.